Electric fields as a means of controlling thin film flow over topography

Sergii VEREMIEIEV [1,*], Philip H. GASKELL [1], Yeaw Chu LEE [1], Harvey M. THOMPSON [1]

* Corresponding author: Tel.: +44 (0)113 3432200; Fax: +44 (0)113 2424611; Email: s.veremieiev@leeds.ac.uk
1: School of Mechanical Engineering, University of Leeds, LS2 9JT, UK

Abstract Gravity-driven, steady-state flow of a thin liquid film over a substrate containing topography in the presence of a normal electric field is investigated. The liquid is assumed to be a perfect conductor and the air above it an ideal dielectric. The Navier-Stokes equations are solved using a new depth-averaged approximation that is capable of analysing film flows with inertia, with the flow coupled to the electric field via a Maxwell normal stress term that results from the solution of Laplace's equation for the electric potential above the film. The latter is solved analytically using separation of variables and Fourier series. The coupled solver is used to analyse the interplay between inertia and electric field effects for flow over one-dimensional step and trench topographies and to predict the effect of an electric field on three-dimensional Stokes flow over a two-dimensional trench topography. Sample results are given which investigate the magnitude of the electric fields needed to suppress free surface disturbances induced by topography in each of the cases considered.
Keywords: Thin liquid films, free surface flow, electrohydrodynamics, numerical solutions, topography.

1. Introduction

This paper considers the flow of thin liquid films over substrates containing topography. Such free surface flows are an important component of numerous manufacturing processes for the production of displays, printed circuits and sensors and, more generally, play an important role in the rapidly evolving area of microfluidics [1]. Several experimental and, more commonly, theoretical studies of the flow which arises have now appeared in the literature, see for example [2-4], and have demonstrated how topography induces both local and non-local disturbances to the film's free surface profile. A key issue within precision manufacturing processes is that these disturbances can persist over length scales far larger than the topographies themselves. In the case of photolithographic manufacture of display screens, for example, this can seriously impair their optical resolution [2].

Previous studies into the control of free surface disturbances induced by topography have focused on flows over one-dimensional features using either: (i) local heating sources to induce Marangoni surface tension gradients [5]; (ii) modifications to the initially flat, non-functional areas of the substrate to mitigate free surface disturbances induced by the functional topography [6]; (iii) visco-elasticity to reduce the amplitude of free surface disturbances [7].

In contrast to the above, the effect of a normal electric field on such film flows is explored, an issue that has been investigated in several experimental and theoretical studies, see for example [8-10]. Of particular relevance is the recent work of Tseluiko and co-workers [11, 12] who solved the Stokes (flow) and Laplace (electric potential) equations, coupled by Maxwell normal stresses at the film's free surface, for flow over one-dimensional topography. The present work incorporates the additional, competing influence of inertia and extends the analysis to three-dimensional flow over two-dimensional topography.

The structure of the paper is as follows. Section 2 presents the mathematical formulation of the problem, while Section 3 outlines the method of solution. Section 4 describes new results for both two- and three-

dimensional flows over topography. Conclusions are drawn in Section 5.

2. Mathematical formulation

Consider the case, shown in Fig. 1, of steady, gravity-driven thin film flow down a planar substrate, containing topography, inclined at an angle θ to the horizontal.

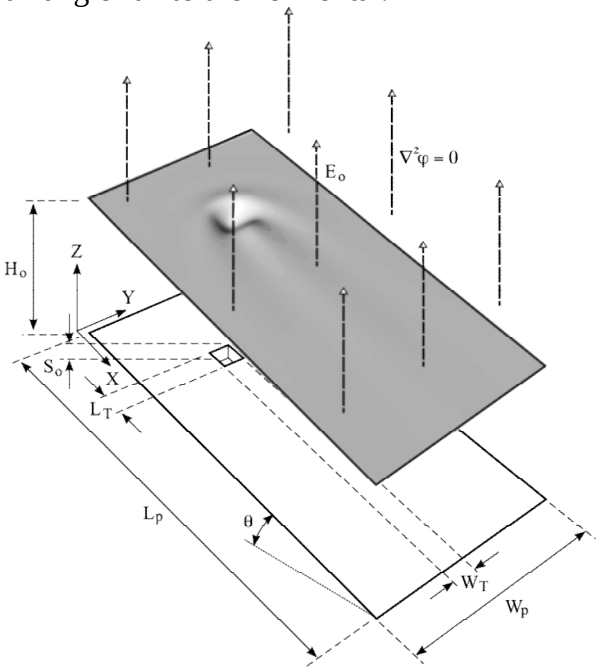

Fig 1: Schematic of gravity-driven flow over a trench topography in the presence of an electric field.

The liquid is assumed to be incompressible with constant density, ρ, viscosity, μ, and surface tension, σ. The film is subjected to a constant, normal electric field, of strength E_0; the air above it is assumed to be a perfect dielectric with constant permittivity ε_e. The electric potential above the film, Φ, satisfies the relation $\underline{E} = -\nabla\Phi$ where $\underline{E}$ is the electric field. The liquid is assumed to be a perfect conductor so that there is no potential difference between the substrate and the free surface and, hence, no electric field in the film.

The governing hydrodynamic equations are the steady-state Navier-Stokes and continuity equations:

$$\rho\left(\underline{U}.\nabla\right)\underline{U} = -\nabla P + \nabla\underline{\underline{T}} + \rho\underline{G}, \quad (1)$$

$$\nabla\cdot\underline{U} = 0, \quad (2)$$

where $\underline{U} = (U,V,W)$ and P are the fluid velocity and pressure, respectively; $\underline{\underline{T}} = \mu\left(\nabla\underline{U} + (\nabla\underline{U})^T\right)$ is the viscous stress tensor, $\underline{G} = g_0(\sin\theta, 0, -\cos\theta)$ is the acceleration due to gravity and g_0 is the gravity constant. The (X,Y,Z) Cartesian coordinates are directed streamwise, spanwise and normal to the substrate plane, respectively and the film is bounded by the substrate $Z = S(X,Y)$, film free surface $Z = F(X,Y)$, inflow plane $X = 0$, outflow plane $X = L_p$ and side planes at $Y = 0$ and $Y = W_p$. The film thickness $H = F - S$ and the values L_p and W_p are taken so as to be large enough to ensure fully developed flow both upstream and downstream.

The length scale is taken as the fully developed asymptotic film thickness, H_0, and velocities and pressure/stresses are scaled with respect to the free surface velocity $U_0 = \rho g_0 H_0^2 \sin\theta / 2\mu$ and average pressure $P_0 = \mu U_0 / H_0$, respectively [13]. This enables equations (1) and (2) to be rewritten as:

$$\mathrm{Re}\left(\underline{u}.\nabla\right)\underline{u} = -\nabla p + \nabla\underline{\underline{\tau}} + \mathrm{St}\,\underline{g}, \quad (3)$$

$$\nabla\cdot\underline{u} = 0, \quad (4)$$

in terms of equivalent non-dimensional (lower case) variables, where the Reynolds number $\mathrm{Re} = \rho U_0 H_0 / \mu$ and the Stokes number $St = 2/\sin\theta$. The problem is closed by imposing appropriate no-slip, inflow, outflow, kinematic and free surface tangential and normal stress boundary conditions, namely:

$$\underline{u}\big|_{z=s} = 0, \quad (5)$$

$$\underline{u}\big|_{x=0,l_p;\, y=0,w_p} = (z(2-z),0,0), \quad (6)$$

$$u\big|_{z=f}\cdot f_x + v\big|_{z=f}\cdot f_y - w\big|_{z=f} = 0, \quad (7)$$

$$\left(\underline{\underline{\tau}}\big|_{z=f}\cdot\underline{n}_f\right).\underline{t} = 0, \quad (8)$$

$$-p\big|_{z=f} + \left(\underline{\underline{\tau}}\big|_{z=f}\cdot\underline{n}\right).\underline{n} = \frac{\kappa}{Ca} + We\,(\nabla\varphi)^2\big|_{z=f}. \quad (9)$$

In equations (5)-(9) the dimensionless electric potential $\varphi = \Phi/H_0E_0$, the unit free surface normal vector pointing towards the air is

$\underline{n} = \left(-f_x, -f_y, 1\right)\left(f_x^2 + f_y^2 + 1\right)^{-1/2}$, $\underline{t}$ is the unit vector tangential to the free surface and $\kappa = -\nabla \cdot \underline{n}$ is the free surface curvature. In the normal stress boundary condition (9), the capillary number $Ca = \mu U_0 / \sigma$ and $We = \varepsilon_e H_0 E_0^2 / 2\mu U_0$ is the Weber number that measures the relative importance of electric and viscous free surface stresses. The appearance of the additional Maxwell stress term for non-zero *We* leads to coupling between the fluid flow and electric field.

2.1 Depth-averaged form (DAF)

The flow is analysed using a new depth-averaged form (DAF) of the Navier-Stokes equations that embodies inertial effects directly. Since a detailed description is given elsewhere [14], only a brief outline is provided below. Equations (3)-(9) are simplified using the long wavelength approximation for $\varepsilon = H_0 / L_0 << 1$, where L_0 is an appropriate in-plane capillary length scale, which is expressed by a transformed set of non-dimensional variables,

$$(x, y, p) \to (x, y, p)/\varepsilon\,, \quad w \to \varepsilon w, \qquad (10)$$

and is formulated in terms of the averaged velocities $\bar{u}(x,y) = \frac{1}{h}\int_s^f u\,dz$, $\bar{v}(x,y) = \frac{1}{h}\int_s^f v\,dz$ and film thickness $h(x,y)$. This enables equations (3) and (4) to be rewritten as

$$\frac{6}{5}\varepsilon\,\mathrm{Re}\left(\bar{u}\bar{u}_x + \bar{v}\bar{u}_y\right) = \left[\frac{\varepsilon^3}{Ca}\nabla^2(h+s) - 2\varepsilon\cot\theta(h+s)\right]_x + \left[\varepsilon We\,\varphi_z^2\big|_f\right]_x - \frac{3\bar{u}}{h^2} + 2\,, \qquad (11)$$

$$\frac{6}{5}\varepsilon\,\mathrm{Re}\left(\bar{u}\bar{v}_x + \bar{v}\bar{v}_y\right) = \left[\frac{\varepsilon^3}{Ca}\nabla^2(h+s) - 2\varepsilon\cot\theta(h+s)\right]_y + \left[\varepsilon We\,\varphi_z^2\big|_f\right]_y - \frac{3\bar{v}}{h^2}\,, \qquad (12)$$

$$\left(h\bar{u}\right)_x + \left(h\bar{v}\right)_y = 0\,, \qquad (13)$$

where the electric stresses at the free surface are obtained by solving Laplace's equation for the electric potential φ (discussed subsequently).

Note that although the DAF equations are valid for non-zero Re, they share the limitation of all long wavelength analyses that they are valid only for small capillary numbers, $Ca = \varepsilon^3 / 6 << 1$.

2.2 Determination of the Maxwell Normal Stress Term

The electric field is obtained by solving $\nabla^2\varphi = 0$ between the inflow and outflow planes $x = 0$ and $x = l_p$, respectively, the side planes at $y = 0$ and $y = w_p$ and the semi-infinite region above the film's free surface. This is achieved subject to the conditions that $\varphi = 0$ at the free surface and uniformity of the electric field at the inflow, outflow and side boundaries and as $z \to \infty$. Following [11], the capillary length L_0 is taken as the length scale in all directions, including normal to the substrate, and the problem is analysed more conveniently using a 'shifted' electric field potential $\tilde{\varphi} = \varphi - 1 + z$ which measures the deviation from a uniform electric field. This satisfies

$$\nabla^2\tilde{\varphi} = 0\,, \qquad (14)$$

subject to the conditions:

$$\tilde{\varphi}\big|_{z=\varepsilon f} = f - 1 \quad \text{and} \qquad (15)$$

$$\nabla\tilde{\varphi}\big|_{x=0,l_p;y=0,w_p;z\to\infty} = 0\,. \qquad (16)$$

The assumption that $\varepsilon << 1$ is used to approximate the free surface boundary condition (16) as:

$$\tilde{\varphi}\big|_{z=0} = f - 1. \qquad (17)$$

The boundary value problem (14), (16) and (17) is solved using the method of separation of variables with $\tilde{\varphi}$ expressed as the following Fourier series:

$$\tilde{\varphi}(x,y,z) = \frac{1}{l_p w_p}\int_0^{l_p}\int_0^{w_p}(f-1)\,d\tilde{x}\,d\tilde{y}\sum_{m,n=0}^{\infty}\cos\left[\lambda_m(x-\tilde{x})\right] \times\cos\left[\mu_n(y-\tilde{y})\right]\exp\left(-\sqrt{\lambda_m^2+\mu_n^2}\,z\right) \qquad (18)$$

with eigenvalues $\lambda_m = m\pi / l_p$ and $\mu_n = n\pi / w_p$. This enables the Maxwell normal stress term to be approximated by:

$$\varepsilon We\,\varphi_z^2\big|_f \approx \varepsilon We + 2\cdot 6^{2/3} We' F\left[f-1\right], \qquad (19)$$

where $F[g]$ is the electric field operator:

$$F[g](x,y)=\frac{1}{l_p w_p}\int_0^{l_p}\int_0^{w_p} g(\tilde{x},\tilde{y})d\tilde{x}d\tilde{y}\sum_{m,n=0}^{\infty}\sqrt{\lambda_m^2+\mu_n^2}\times\cos[\lambda_m(x-\tilde{x})]\cos[\mu_n(y-\tilde{y})] \quad (20)$$

and $We'=Ca^{2/3}We$ is the modified Weber number. Specifying the values of Re and We' in the above leads to the following asymptotic film thickness, capillary number and electric field strength, respectively:

$$H_0=\left(\frac{2\mu^2}{\rho^2 g_0\sin\theta}\right)^{1/3}\mathrm{Re}^{1/3}, \quad (21)$$

$$Ca=\left(\frac{g_0\mu^4\sin\theta}{2\rho\sigma^3}\right)\mathrm{Re}^{2/3}, \quad (22)$$

$$E_0=\left(\frac{32\sigma^6\rho^5 g_0^4\sin^4\theta}{\mu^2\varepsilon_e^9}\right)^{1/18}\frac{We'^{1/2}}{\mathrm{Re}^{1/18}}. \quad (23)$$

2.3 Topography Definition

Attention is restricted to flow over simple one-dimensional trench, step-up and step-down topography and in two-dimensions a localized rectangular trench. Following previous studies [15], topography is specified using arctangent functions. For one-dimensional trench topography this takes the form:

$$s(x^*)=\frac{s_0}{\tan^{-1}(l_t/2\delta)}\left[\tan^{-1}\left(\frac{x^*+l_t/2}{\delta}\right)-\tan^{-1}\left(\frac{x^*-l_t/2}{\delta}\right)\right], \quad (24)$$

where s_0, l_t and δ are the dimensionless depth, width and steepness of the topography. For both one- and two-dimensional topography the in-plane coordinates $(x^*,y^*)=(x-x_t,y-y_t)$ are shifted to the center of the topography, (x_t,y_t). More complex topography can be defined similarly [4].

3. Method of solution

The depth-averaged equations (11) - (13) are solved on a uniform, rectangular computational domain, $(x,y)\in(0,l_p)\times(0,w_p)$ subdivided using a staggered mesh arrangement with a total of $n_x\times n_y$ cells, each of length $\Delta x=l_p/n_x$ and width $\Delta y=w_p/n_y$. The unknown variables, h, and velocity components $\bar{u}$ and $\bar{v}$ are located at cell centres (i,j) and cell faces $(i+1/2,j)$ and $(i,j+1/2)$, respectively. The momentum equations (11), (12) are solved at cell faces and the continuity equation (13) at cell centres using a second order accurate finite difference scheme [14].

Following [11] the discretisation involves the use of ghost nodes, where the solution is found by the assumption of its periodicity in both the x and y directions:

$$(\bar{u},\bar{v},h)\big|_{x\pm l_p}=(\bar{u},\bar{v},h)\big|_x, \quad (25)$$

$$(\bar{u},\bar{v},h)\big|_{y\pm w_p}=(\bar{u},\bar{v},h)\big|_y, \quad (26)$$

and for the unique determination of the solution the film thickness is fixed at the inflow:

$$h\big|_{x=0}=1. \quad (27)$$

The topography function has to satisfy the periodicity conditions stated above as well, therefore a wide trench is used to investigate free surface disturbance over step-up and step-down features.

Discretization of the electric field operator is implemented by defining the tensor:

$$F_{i,j,k,l}=\frac{1}{n_x n_y}\sum_{m,n=0}^{N^f}\sqrt{\lambda_m^2+\mu_n^2}\cos\frac{m\pi(i-k)}{n_x}\cos\frac{n\pi(j-l)}{n_y},$$

which accounts for the action of the operator $F[g]_{i,j}=F_{i,j,k,l}g_{k,l}$. Here the associated integrals are evaluated numerically using the trapezoidal quadrature rule and the number of Fourier terms N^f is chosen to be sufficiently large to ensure convergence. Note that the symmetry of the operator is exploited to store only $(n_x+1)(n_y+1)$ elements of the operator that correspond to all possible magnitudes of differences $|i-k|$ and $|j-l|$. These are created once, at the beginning of the calculation, and used for all iterations thereafter.

The $n_x\times n_y$ mesh cells lead to a total of $3(n_x+1)(n_y+1)$ discretised equations. These

are linearised by the Newton-Raphson method and solved directly by LU decomposition with partial pivoting utilising the associated subroutine in the freely available LAPACK library [16]. The latter reduced residuals below 10^{-6}, typically within 4-5 iterations.

4. Results

Following previous studies [2, 4, 11], attention is restricted to flow over simple step and trench topographies for gravity-driven flow of thin water films in air, with ρ = 1000 kg·m^{-3}, μ = 10^{-3} Pa·s, σ = 0.07 N·m^{-1}, ε_e = 8.85·10^{-12} F·m^{-1} and θ = 30º. Topography is specified with δ = 0.001, a value small enough to ensure that solutions are independent of steepness; N^f = 200 Fourier terms are found to be sufficient in all cases. The topography and free surface coordinates are presented in terms of the depth of the topography: $s^* = s/s_0$, $f^* = (f-1)/s_0$.

Fig. 2 shows the effect of an electric field on the free surface profiles of flows over the one-dimensional step topographies considered experimentally by [2] that are approximated by a wide trench with l_t = 80, s_0 = 0.2, Re = 2.45, H_0 = 100μm, x_t = 120 and l_p = 200. In order to resolve small oscillations on the free surface upstream of the steps [11] the domain is meshed finely with n_x = 4096 cells.

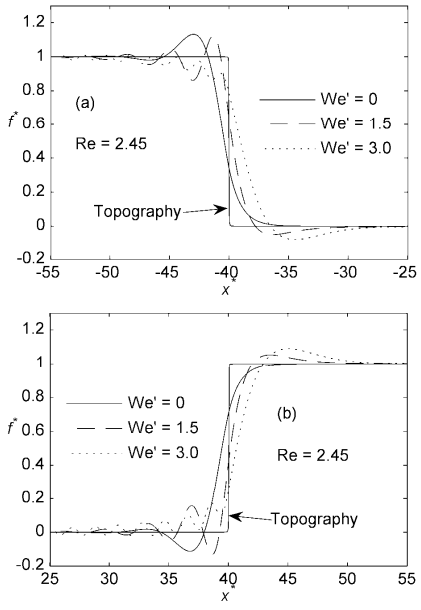

Fig 2: Effect of We' on free surface profiles for flow over (a) step-down, (b) step-up with $|s_0|$= 0.2, Re=2.45 and θ= 30º.

Fig 2(a) shows how increasing *We′* (and hence the Maxwell normal stress) causes a downstream displacement of the free surface disturbance, resulting in a thickening of the film over the step-down and reducing the magnitude of the capillary ridge. For the step-up case, Fig 2(b), a downstream displacement with increasing *We′* is also observed, causing the disappearance, of the upstream depression and the formation of a capillary ridge downstream of the step-up. In both cases, increasing *We′* leads to the creation of an oscillatory free surface upstream of the topography, as observed in the recent studies of [11, 12]. These are created by the additional Maxwell stresses which are balanced by increased capillarity/curvature.

Figure 3 shows the effect of *We′* on flow over the topographies considered in Fig. 2 when Re is increased to 30 (H_0 = 231μm).

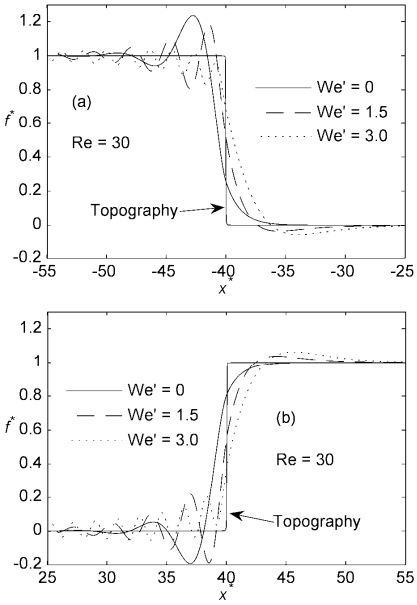

Fig 3: Effect of We' on free surface profiles for flow over (a) step-down, (b) step-up with $|s_0|$=0.2, Re=30 and θ=30º.

These shows how inertia generally amplifies the free surface disturbances [14] and that larger electric fields are needed to suppress the associated free surface disturbances. For

example, for flow over the step-down, increasing We' to 3 leads to complete suppression of the capillary ridge for $\mathrm{Re} = 2.45$, whereas for $\mathrm{Re} = 30$ a small free surface overshoot remains.

The effect of an electric field on the free surface profile for flow over the one-dimensional trench considered experimentally by [2], with width $l_t = 1.51$, depth $s_0 = 0.19$, $\mathrm{Re} = 2.84$, $H_0 = 105\mu\mathrm{m}$, $x_t = 50$, $l_p = 100$ and $n_x = 2048$, is shown in Fig. 4.

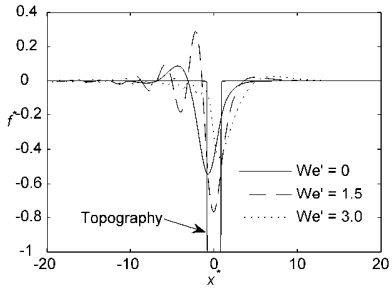

Fig 4: Effect of We' on free surface profiles for flow over trench with l_t=1.51, s_0=0.19, Re=2.84 and $\theta=30^o$.

The effect of We' is very different in this case since increasing We' to 1.5 leads to a significant amplification of the capillary ridge upstream of the trench and a corresponding increase in the free surface depression over the trench, while increasing We' further to 3.0 leads to a gradual suppression of the free surface disturbances. This behaviour may be due to the interaction between waves associated with the step-down/-up components of the trench.

The final example extends the analysis to consider the effect of an electric field on flow over the two-dimensional square trench topography used by [2] with width and length $l_t = w_t = 1.54$, depth $s_0 = 0.25$, $\mathrm{Re} = 2.45$, $H_0 = 100\mu\mathrm{m}$, $x_t = y_t = 50$, and $l_p = w_p = 100$. Due to the excessive computational cost of solving electrified three-dimensional flow for $\mathrm{Re} > 0$, solutions are given for the Stokes flow case only, solved using a lubrication approach, as described by [4], for which $n_x = n_y = 256$ cells yield grid-independent solutions.

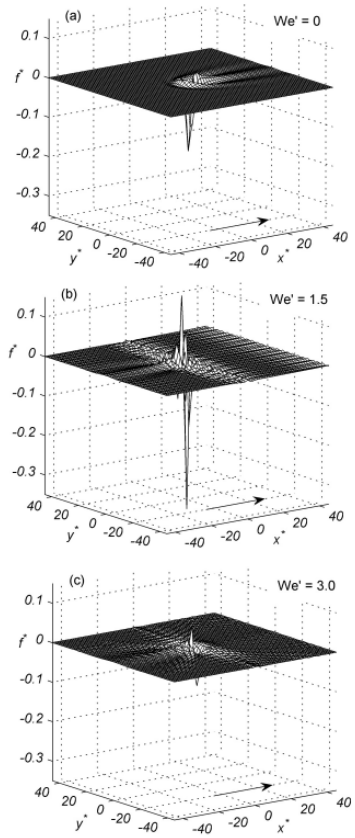

Fig. 5: Three-dimensional free surface profiles for Stokes flow over a two-dimensional rectangular trench with l_t=w_t=1.54, s_0=0.25, Re= 2.45 and $\theta=30^o$. The arrow shows the direction of flow.

As for the one-dimensional trench, free surface disturbances are amplified for We' =1.5 and suppressed for We' =3.0. This is seen more clearly in Fig. 6, which shows plots of streamwise and spanwise free surface profiles through the centre of the topography.

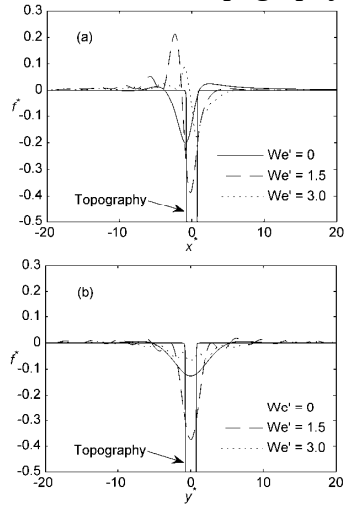

Fig 6: Effect of We' on (a) streamwise and (b) spanwise free surface profiles for Stokes flow over a two-dimensional rectangular trench.

5. Conclusions

Inertial thin film flow over various one- and two-dimensional topography in the presence of an electric field normal to the free surface has been investigated by means of a novel approach comprised of utilising and solving a depth averaged form of the governing hydrodynamic equations, with the coupled electric potential above the film determined analytically using separation of variables and a Fourier series representation. The generation of accurate, steady-state, mesh independent solutions to the coupled equation set is realised by employing a staggered grid arrangement for the dependent hydrodynamic variables together with proper treatment of the nonlinear convective terms present.

The results obtained show that for inertial flow over one-dimensional simple step topography, the size of capillary ridges and depressions decrease with increasing electric field strength, while stronger fields are needed to suppress the larger free surface disturbances that occur as a consequence of increasing inertia. In the case of flow over a one-dimensional trench topography, the behaviour is more complex since increasing the strength of the electric field initially amplifies disturbances, which is followed by their suppression at higher field strengths. The subtle interplay that occurs between electric field strength, inertia and topography geometry suggests the problem is worthy of a subsequent more detailed parametric study.

In the case of flow over two-dimensional topography the results obtained were restricted to the special case of Stokes flow since the computational memory required to accurately resolve three-dimensional flows in the presence of an electric field when the Reynolds number is non-zero is currently too prohibitive – the principal reason being the need to solve a dense matrix system of integro-differential equations. Measures to overcome these restrictions, such as using a parallel computing framework, are currently being persued.

6. Acknowledgements

S. Veremieiev gratefully acknowledges the financial support of the European Union via Marie Curie Action Contract MEST-CT-2005-020599.

References

1. Tabeling, P., *Introduction to Microfluidics*. 2005, Oxford: Oxford University Press.
2. Decre, M.M.J. and J.C. Baret, *Gravity-driven flows of viscous liquids over two-dimensional topographies.* Journal of Fluid Mechanics, 2003. **487**: p. 147-166.
3. Kalliadasis, S., C. Bielarz, and G.M. Homsy, *Steady free-surface thin film flows over topography*. Physics of Fluids, 2000. **12**(8): p. 1889-1898.
4. Gaskell, P.H., et al., *Gravity-driven flow of continuous thin liquid films on non-porous substrates with topography.* Journal of Fluid Mechanics, 2004. **509**: p. 253-280.
5. Gramlich, C.M., et al., *Optimal leveling of flow over one-dimensional topography by Marangoni stresses.* Physics of Fluids, 2002. **14**(6): p. 1841-1850.
6. Sellier, M., *Substrate design or reconstruction from free surface data for thin film flows.* Physics of Fluids, 2008. **20**(6).
7. Saprykin, S., R.J. Koopmans, and S. Kalliadasis, *Free-surface thin-film flows over topography: influence of inertia and viscoelasticity.* Journal of Fluid Mechanics, 2007. **578**: p. 271-293.
8. Kim, H., S.G. Bankoff, and M.J. Miksis, *The effect of an electrostatic field on film flow down an inclined plane.* Physics of Fluids A: Fluid Dynamics, 1992. **4**(10): p. 2117-2130.
9. Gonzalez, A. and A. Castellanos, *Nonlinear electrohydrodynamic waves on films falling down an inclined plane.* Physical Review E, 1996. **53**(4): p. 3573-3578.
10. Griffing, E.M., et al., *Electrohydrodynamics of thin flowing films.* Journal of Fluids Engineering-Transactions of the Asme, 2006. **128**(2): p. 276-283.
11. Tseluiko, D., et al., *Electrified viscous thin film flow over topography.* Journal of Fluid Mechanics, 2008. **597**: p. 449-475.
12. Tseluiko, D., et al., *Effect of an electric field on film flow down a corrugated wall at zero Reynolds number*. Physics of Fluids, 2008. **20**(4).
13. Spurk, J.H. and N. Aksel, *Fluid mechanics*. 2008: Springer.
14. Veremieiev, S., et al., *Computing inertial two-*

and three-dimensional thin film flow on planar surfaces featuring topography. submitted to the Computers & Fluids, 2009(www.efm.leeds.ac.uk~menhmt/papers/jcompphys/paper2009.pdf).

15. Stillwagon, L.E. and R.G. Larson, *Fundamentals of Topographic Substrate Leveling*. Journal of Applied Physics, 1988. **63**(11): p. 5251-5258.
16. Anderson, E., et al., *LAPACK Users' Guide*. Society for Industrial and Applied Mathematics, 1999.